MGPB

Algerian northwestern seismic hazard evaluation based on the Markov model

The Mining-Geology-Petroleum Engineering Bulletin
UDC: 550.3
DOI: 10.17794/rgn.2019.1.10

Review professional paper

Badreddine Dahmoune[1]; Hamidi Mansour[1]
[1] *Laboratoire Géo-ressources, Environnement et Risques Naturels, Université d'Oran 2 Mohamed Ben Ahmed, Algérie*

Abstract
The main aim of this paper is to develop a markovienne model for the evaluation of seismic hazard in the north-western part of Algeria. A region that accommodates from moderate to strong seismic activity ($M_L \geq 2.5$). This work is an attempt to conceive a stochastic model of the earthquake occurrences in order to assess the seismic hazard based on the use of a discrete time Markov chain with a finite state model. The presented model is applied on a complete data sample comprising most of the earthquakes that occurred in the Algerian northwestern area located between latitudes (34°N, 37°N) and longitudes (2°W, 3°E) since 1928 up to now (2018). The Markov chain is built over a homogeneous and completed catalogue, then the transition probability matrix of the chain is used to simulate the occurrences of the earthquakes in the coming decades. The results are compared to a classic Poisson model.

Keywords:
Seismic hazards, Markov chain, Poisson model, earthquake, North Algeria.

1. Introduction

Algeria is located in the northern part of the African plate facing the Eurasian plate. Thus, the northwestern region of Algeria is stuck between the Nubian and Eurasian tectonic plates with a very complex boundary between them, which is converging along a N-S to NNW-SSE direction since at least the early Quaternary period **(McKenzie, 1972), (Philip, 1987)**. Based on paleo-seismological data **(Meghraoui, 1988)** and on the study of source mechanisms **(Meghraoui et al., 1996)** the motion rate is evaluated 4-6 mm per year. This convergence geodynamic process produces a large band of about 100-150 km, composed of Neogene deposits and deformed quaternary, comes into sight in the northern region of Algeria as the Tellian chain **(Philip and Thomas, 1977)**, **(Philip and Meghraoui, 1983), (Thomas, 1985)**. More precisely, the Tellian chain is formed by folds lying NE-SW which are organized in an echelon system, probably caused by the presence of deep E-W strikes slip **(Bouhadad and Laouami, 2002).** When compared to other countries in North Africa, the seismicity of Algeria is moderate to strong, scattered and concentrated in its northern part. Seismic activity is induced by Nubian-Eurasian convergence accumulated particularly in the Tellian chain, where the coastal part of this chain is the most active **(Déverchère et al., 2005).** According to historical documents and instrumental measurements, several strong earthquakes took place within the north border of the country.

Thus, a considerable amount of seismic activity observed in the northwest of Algeria is due to the convergence area between the Eurasian and African plates. An important number of shakes recorded during the last decades have been highly felt, and a number of them have been damaging, for instance the Oran earthquake of October 9, 1790 of intensity X (MSK scale), where about 3,000 human lives were claimed **(Buforn et al., 2017)**, and the Beni-Chougrane August 18, 1994 earthquake of intensity VIII (M_s **= 5.6**), which caused 171 deaths, and the collapse of about 1,000 constructions **(CGS, 1995).** Recall also the 1980 El-Asnam earthquake which occurred on October 10 at 13:25:25 local time with a surface wave magnitude of M_s **=7.3**. It was the largest earthquake in Algeria, and was followed three hours later by an aftershock of magnitude 6.2. Both events caused considerable damage with at least 2,600 killed and 8,300 injured **(Dewey, 1991).** This history shows that the northwestern region of Algeria is exposed to significant seismic risk and is considered as an active area in Algeria. Especially the fact that this region includes the city of Oran, the largest and the most populated city in the northwestern region of Algeria.

This paper presents a discrete-time Markov chain to model the seismic activity in northwestern region of Algeria in order to infer the past seismic events to evaluate probabilistic earthquake forecasting results. The transition probabilities of the chain are estimated along with

Corresponding author: Badreddine Dahmoune
dhbadro@gmail.com

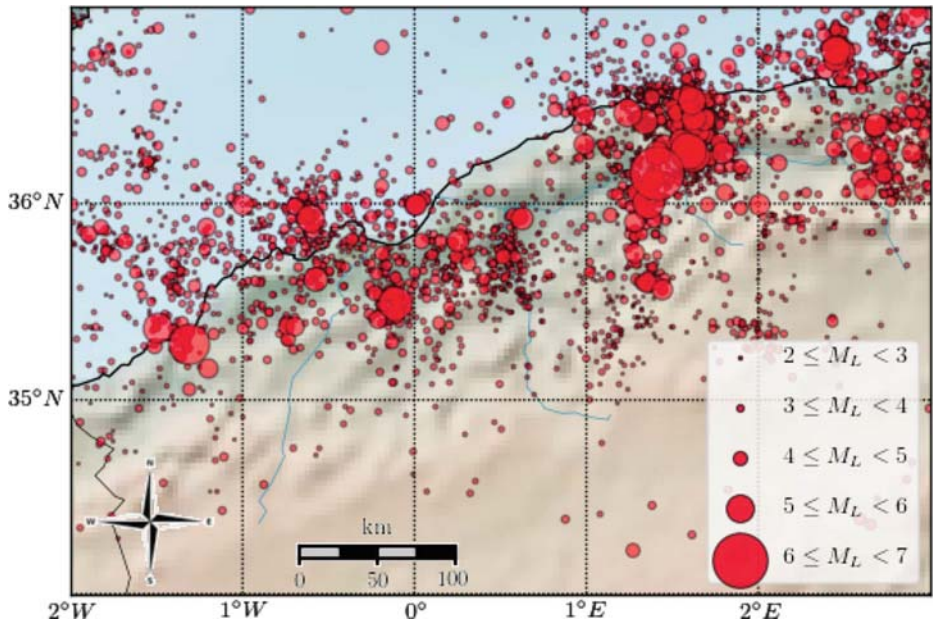

Figure 1: Seismicity map of Northwestern Algeria from the compiled homogeneous catalogue of the period between 1928 and 2018 (see **Section 3**)

its relevant measures, resulting in the calculation of earthquake occurrence probabilities. The model is based on the local magnitude, date, time, and epicenter location of each past seismic event.

The rest of this paper is organized as follows. **Section 2** presents the methodology and details of all the elements of the suggested model. After that, **Section 3** describes and analyses the data set that will be used. It includes the homogenization and the completeness of the data. Then, **Section 4** explains how the studied region is divided into two principal zones. Next, **Section 5** justifies the choice of a time unit of 248 days to sample the seismic event data of the compiled catalog. Finally, **Section 6** discusses the obtained results based on the Markov chain.

2. Methodology

The use of probabilistic methods in the study of seismic activity has been greatly considered in literature. Several studies show that two main methods are used: the Poisson process that is more adapted to frequent events **(Cornell, 1968), (Cornell and Vanmarcke, 1969), (Schenková and Kárník, 1970), (Liu and Fagel, 1972), (Merz and Cornell, 1973), (Caputo, 1974), (Der Kiureghian and Ang, 1977)**, and the Markov process which is adapted for the analysis of less frequent random events **(Vagliente, 1973), (Veneziano and Cornell, 1974), (Lomnitz-Adler, 1983),** and more recently **(Beyreuther and Wassermann, 2008), (Beyreuther et al., 2012), (Votsi et al., 2013), (Quang et al., 2015).** The choice of the Markov model for the analysis of seismic risk is based on the fact that, in general, an earthquake is a direct result of the earthquake that precedes it **(Vere-Jones, 1966), (Knopoff, 1971).** Additionally, as enough data is available nowadays, methods based on pattern-recognition are recently very popular among research work **(Peresan et al., 2005).**

Moreover, scholars active in this field, as exact prediction is extremely difficult, are only trying to estimate a probable time, a probable location, and a probable magnitude in which a future event is likely to happen. Therefore, research on methods of prediction focus on empirical data analysis, with two principal approaches:

1. Identifying distinctive precursors to earthquakes: with potential utility for short-term earthquake prediction or forecasting. These methods include the analysis of: animal behaviour **(Lott et al., 1981; Bhargava et al., 2009),** the dilatancy-diffusion model **(Anderson and Whitcomb, 1973; Nur, 1974),** changes in the ratio between the primary and the secondary velocities **(Nicholson and Simpson, 1985; Wang et al., 1975)**, gas emissions **(King, 1986; Heinicke et al., 1995; Chyi et al., 2003; Walia et al., 2005),** and electromagnetic anomalies **(Eftaxias et al., 2001; Uyeda et al., 2009).**
2. Identifying some kind of geophysical trend or pattern in seismicity that might precede a large earthquake: generally thought to be useful for forecasting from intermediate to long term prediction (from one year to a century time scale). These approaches are based on the analysis of: elastic rebound **(Matthews et al., 2002),** characteristic earthquakes **(Aki, 1984; Bakun and Lindh, 1985; Jackson and Kagan, 2006),** seismic gaps **(Rong et al., 2003; Seeber and Armbruster, 1981)**, and

seismicity patterns **(Mogi, 1981; Holliday et al., 2005)**.

The method described here is based mainly on the use of the Markov approach for the analysis of seismic events. This method essentially uses the closest event to estimate when the event will happen in the future.

One of the goals of seismic activity analysis of a region is to predict future earthquakes. Thus, building a Markov chain based on the seismic events of the past allows a probabilistic prediction of future events **(Serpil and Celebioglu, 2011), (Chambers et al., 2012), (Chen and Liu, 2013), (Votsi et al., 2013).**

The following subsections detail the elements and the necessary parameters used to construct the Markov chain associated with the studied region.

This section introduces the theoretical concept of the Markov chain. Markov processes are named after their discoverer, Andreï Markov **(Markov, 1906)**. A Markov process is a stochastic process having the property to predict the future only by knowing the present. The choice of this model for the analysis of seismic risk is based on the fact that, in general, an earthquake is a direct result of the earthquake that precedes it **(Vere-Jones, 1966), (Knopoff, 1971)**. The following sections focus on the Markov chain in discrete time on a discrete state space.

A discrete time Markov process is a sequence $X_0, X_1, \ldots X_t$ of random variables with values in the state space E. The characteristic property of a Markov chain is: predicting the future from the present cannot be more precise by considering the past, because all the useful information for the prediction of the future is contained in the present state of the process. In general, this property is expressed by the following formula:

$$\forall t \geq 0,\ \forall (e_0, \ldots, e_t, e) \in E^{t+2}: \quad (1)$$

$$Pr\,(X_{t+1} = e \mid X_0 = e_0, \ldots, X_t = e_t) = \\ = Pr\,(X_{t+1} = e \mid X_t = e_t) \quad (2)$$

Where ***Pr*** denotes the probability of an event.

It is assumed that most often Markov chains are homogeneous, i.e. the transition mechanism does not change over time. The homogeneity property is expressed as follows:

$$\forall t \geq 0,\ \forall (e,é) \in E^2: \quad (3)$$

$$Pr\,(X_{t+1} = é \mid X_t = e) = Pr\,(X_1 = é \mid X_0 = e) \quad (4)$$

Notice that only homogeneous Markov chains are considered in this work. Let ε be the magnitude threshold from which a seismic event is taken into account or not. Let H be a seismic catalogue for a given region R. And H is the list of all the seismic events observed in the region R during a period let's say T. Each seismic event v is represented by its position p_v, its magnitude M_v, and the date of its occurrence t_v.

The period T should be divided into identical units of time, during which the seismic activity is observed. The time unit is denoted as Δt. Assume that the studied region is divided into n zones $z_1, z_2, \ldots, z_n$. Thus the region R can be seen as a system of n zones. During the time unit Δt, each zone has two possible states, either 0 or 1:

- $z_i = 0$ if the i-th zone is seismically quiet during the time interval Δt: all the magnitudes of seismic events observed during Δt are strictly lower than the threshold magnitude ε.
- $z_i = 1$ if the i-th zone is seismically active during the time interval Δt: at least one seismic event with a magnitude greater than or equal to the threshold magnitude ε was observed during the time unit Δt.

Thus, the overall state of the region R during Δt is a combination of the states of the n zones: $e = [z_1, z_2, \ldots, z_n]$. This implies that $e \in E = \{0,1\}^n$ and the number of possible global states of the region R is $|E| = 2^n$. In this case, the model is a Markov chain C composed of 2^n states. Each state of the Markov chain represents an overall state of the region R. Therefore, E is the state space of the Markov chain. The transitions between these states are probabilities that must be estimated from the seismic history H. As well, $\theta_{eé}$ denotes how often during the period T, the global state e has been observed during a unit of time, followed by the observation of the global state $é$ during the following unit of time:

$$\theta eé = \#\{(X_t, X_{t+1}) \mid 0 \leq t < T \\ \text{and } X_t = e \text{ and } X_{t+1} = é\} \quad (5)$$

This allows to calculate the probability of transition from the global state e to the global state $é$:

$$Pr(é \mid e) = Pr(X_{t+1} = é \mid X_t = e) = \frac{\theta_{eé}}{\sum_{s \in E} \theta_{es}} \quad (6)$$

The set of all transition probabilities is gathered in a matrix A of size 2^n X 2^n called the transition matrix which is defined as follows:

$$\forall (e,é) \in E^2: A[e, é] = Pr(é \mid e) \quad (7)$$

The Markov chain is well defined by its state space and its matrix of transitions:

$$C = (E, A) \quad (8)$$

Given a seismic catalogue H for a region R over a period T, and R need to be partitioned into n zones. It is necessary also to define a threshold magnitude ε from which a seismic event is considered as important. And as this work considers discrete Markov chains, a time interval Δt to sample the period T should be set.

3. Data set

Despite the fact that earthquake catalogs cover a much shorter period of time compared to paleoseismological periods, the earthquake records are indispensable

Table 1: Distribution of the seismic events on the different catalogue sources

	CRAAG	MDD	CSEM	LDG	ISC	NEIC	IDC	CNRM	INMG	MOS	Other	**Total**
From	2004	1964	1994	1979	1954	1985	2000	1992	2002	1980	1928	1928
To	2016	2018	2018	2018	2015	2018	2018	2013	2018	2018	2018	2018
M_L	2179	194	834	308	1	8	100	84	130	-	212	**4050**
M_b	4	924	214	1	231	109	99	-	7	74	280	**1943**
M_n	-	772	-	-	-	138	-	-	-	-	-	**910**
M_w	-	278	5	-	-	9	-	5	-	-	78	**375**
M_s	-	-	-	10	83	8	63	-	-	32	63	**259**
M_d	-	3	9	4	-	7	-	56	2	-	18	**99**
Total	**2183**	**2171**	**1062**	**323**	**315**	**279**	**262**	**145**	**139**	**106**	**651**	**7636**

for seismic hazard evaluation. This study uses earthquake data from the instrumental period from 1928 to 2018. Data was compiled from fifty different sources and catalogs, which include principally **CRAAG** (Centre de Recherche en Astronomie, Astrophysique et Géophysique, Algéria), **MDD** (Instituto Geográfico Nacional, Spain), **CSEM** (Centre Sismologique Euro-Méditerranéen, France), **LDG** (Laboratoire de Détection et de Géophysique, CEA, France) **ISC** (International Seismological Centre, U.K), **NEIC** (National Earthquake Information Center, U.S.A), **IDC** (International Data Centre, Vienna), **CNRM** (Centre National de Recherche, Morocco), **INMG** (Instituto Português do Mar e da Atmosfera, Portugal), **MOS** (Geophysical Survey of Russian Academy of Sciences, Russia), and from published literature. These catalogs use different parameters such as magnitude scales (M_L: local magnitude, M_b: body wave magnitude, M_n: Nuttli magnitude M_w: moment magnitude, M_s: surface wave magnitude, M_d: duration magnitude), origin time, epicenter and depth information of the earthquakes.

3.1. Homogenization

A homogeneous earthquake catalog with a uniform magnitude scale for measuring the size of past earthquakes is a prerequisite for an accurate evaluation of seismic hazard. **Table 1** shows a total of 7636 records where more than 53% of the records are expressed in terms of the local magnitude M_L. Thus, in this work, all other magnitudes will be converted to the local magnitude. To do so, events of the catalog where several magnitude scale measurements were given for the same event need to be considered. For instance, there are 764 events for which, at the same time, the body wave magnitude M_b and the local magnitude M_L were given. The relationship between M_b and M_L given by **(Benouar et al., 1994)** (for the Ibero-Maghreb region) and by **(Kramer, 1996)** tend to underestimate local magnitude for small body wave magnitudes and tend to overestimate local magnitude for big body wave magnitudes. In fact, a linear regression (minimizing the least squares method) was applied to quantify an empirical relationship between M_b and M_L for the region of study. The same procedure was applied to convert other magnitude scales into the local magnitude when avoiding less accurate conversion relationships given in literature as the **(Sonley and Atkinson, 2005)** formula for Nuttli magnitude or the **(Brumbaugh, 1989)** formula for duration magnitude. The new empirical relationships (see **Figures 2, 3, 4, 5,** and **6**) among M_b, M_s, M_w, M_n, and M_d are formulated as:

$$M_L = 0.812M_b + 0.377 \qquad R^2 = 0.576 \qquad (9)$$

$$M_L = 0.383M_s + 2.951 \qquad R^2 = 0.512 \qquad (10)$$

$$M_L = 0.642M_w + 1.536 \qquad R^2 = 0.644 \qquad (11)$$

$$M_L = 0.988M_n + 0.437 \qquad R^2 = 0.658 \qquad (12)$$

$$M_L = 1.201M_d - 0.689 \qquad R^2 = 0.508 \qquad (13)$$

3.2. Completeness

A look at catalog records shows that the magnitude distribution of events is not homogeneous over time. Thus, to determine the mean rates of occurrence λ, from the entire period (1928-2018) leads to serious underestimations of λ for the middle and low magnitudes. However, if the sample is shortened to the time interval in which the lowest magnitudes included in the computation of λ are completely reported, mean rates of occurrence cannot be established for the largest observed earthquakes because of lack of data. To overcome this problem, the approach suggested by **(Stepp, 1972)** was applied to determine the interval in a magnitude class over which the class is complete.

The earthquake data is grouped into four magnitude classes such as: $M_L < 3$, $3 \leq M_L < 4$, $4 \leq M_L < 5$, and $M_L \geq 5$. With a time interval of one year, the average number of events per year in each magnitude range is determined. If k_1, k_2, ..., k_n are the number of events per year in a magnitude range, then the mean rate for this sample is: $\lambda = \frac{1}{n}\sum_{i=1}^{n} k_i$ where n is the number of unit time intervals. The variance is given by: $\sigma_\lambda = \frac{\lambda}{T}$ where T is the duration of the sample. If λ is constant, σ_λ would vary as $\frac{1}{\sqrt{T}}$.

Thus the standard deviations of the mean rate for the four magnitude intervals as a function of sample length are plotted along with nearly tangent lines with slope $\frac{1}{\sqrt{T}}$.

The deviation of standard deviation of the estimate of the mean from the tangent line indicates the length up to which a particular magnitude range may be taken as complete. The standard deviation shows stability in shorter windows for smaller earthquakes and in longer time windows for large-magnitude earthquakes. The last graph of Figure 7 shows a typical completeness test, with the standard deviation of the estimate of the mean of the annual number of events as a function of sample length for the catalogue.

As presented in **Table 2**, the analysis shows that data is complete for the slices $M_L<3, 3\leq M_L<4$, $4\leq M_L<5$ and $M_L\geq 5$ for the past 15, 20, 50, and 90 years, respectively.

Table 2: Completeness interval for the northwestern region of Algeria

Magnitude class	Period of completeness	Duration
$1\leq M_L<3$	2003-2018	15 years
$3\leq M_L<4$	1998-2018	20 years
$4\leq M_L<5$	1968-2018	50 years
$5\leq M_L$	1928-2018	90 years

3.3. Threshold magnitude of completeness

After dividing the seismic data, the threshold magnitude of completeness M_c, defined as the lowest magnitude above which all events in a given region are detected, is found from the complete part of the catalog.

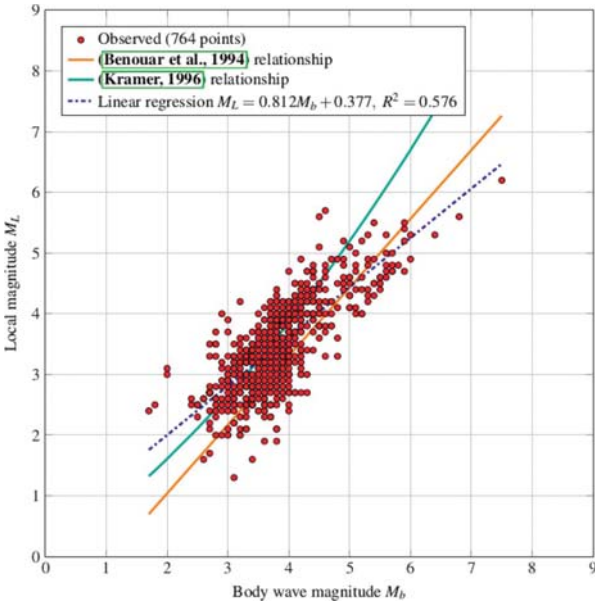

Figure 2: Empirical relationship between body wave magnitude and local magnitude

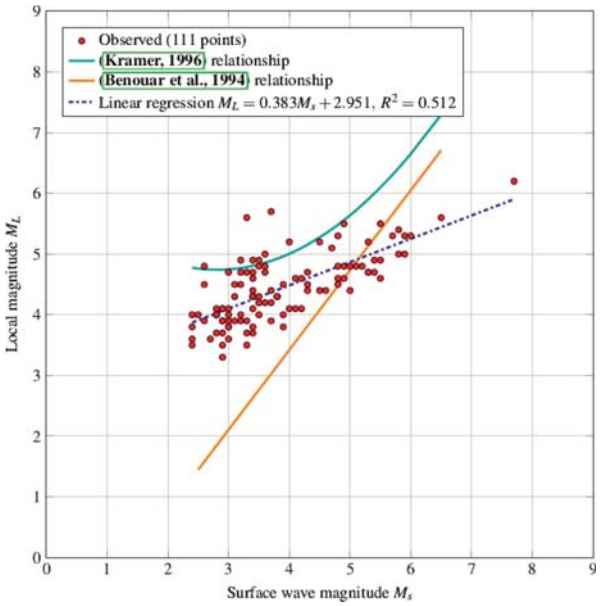

Figure 3: Empirical relationship between surface wave magnitude and local magnitude

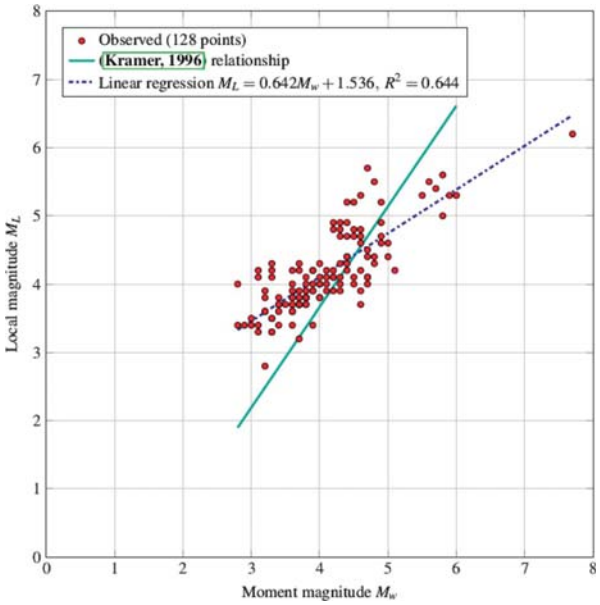

Figure 4: Empirical relationship between moment wave magnitude and local magnitude

The M_c is obtained through regression analysis from the frequency magnitude distribution as the value where the data departs from a straight line **(Wiemer and Wyss, 2000)**. **Figure 8** expresses the relationship between the magnitude and frequency of earthquakes in the considered region.

The threshold magnitude of completeness obtained from the complete part is seen to be around 2.5. Thus,

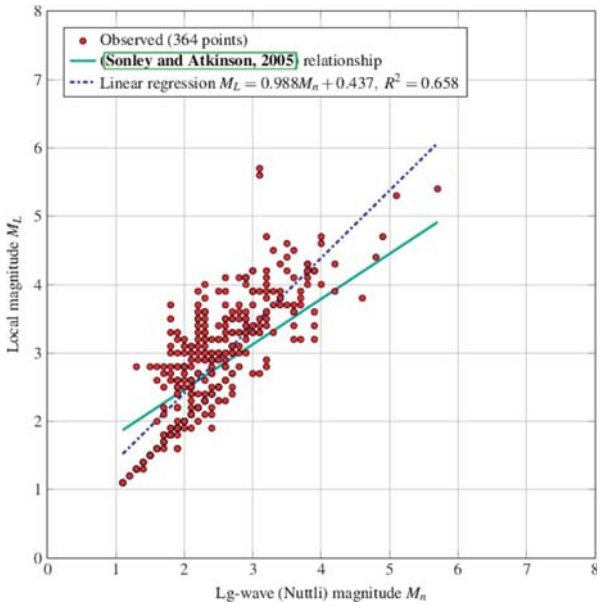

Figure 5: Empirical relationship between Nuttli wave magnitude and local magnitude

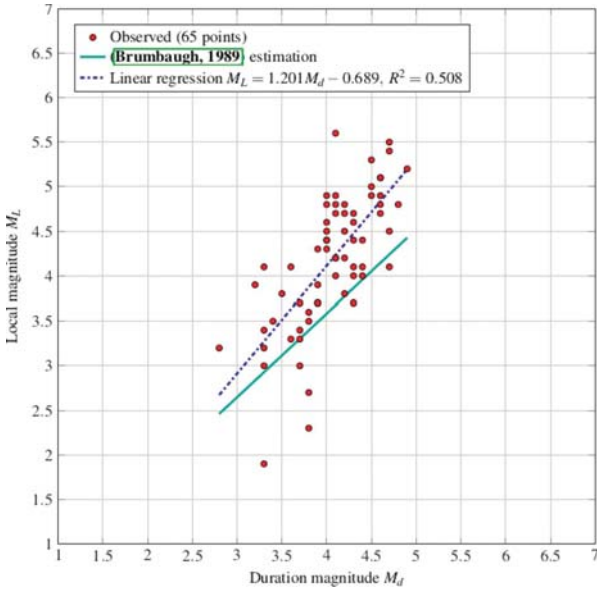

Figure 6: Empirical relationship between duration wave magnitude and local magnitude

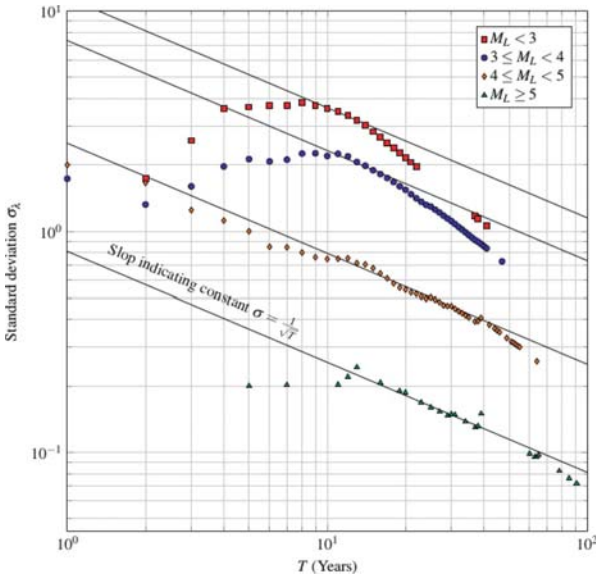

Figure 7: Completeness analysis based on the **(Stepp, 1972)** method

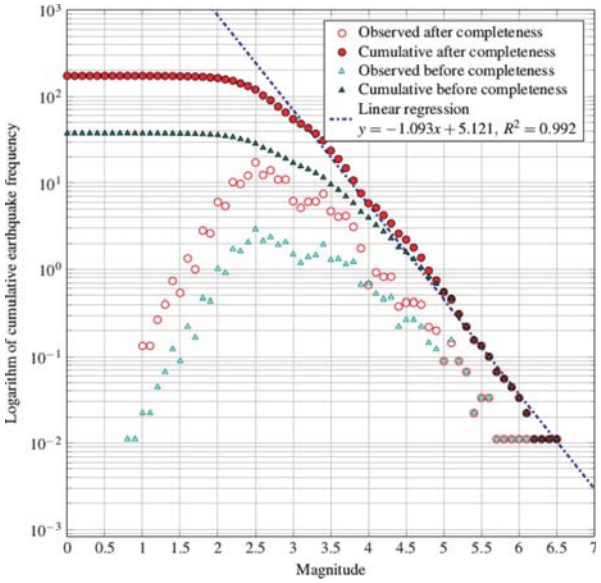

Figure 8: Gutenberg Richter law for Northwestern Algeria. The relationship between the magnitude and frequency of earthquakes in the considered region is used to find the threshold magnitude M_c.

the value of the local magnitude threshold of completeness was chosen as $\boldsymbol{M_c = 2.5}$.

4. Spatial analysis

The studied region in this paper, noted *R*, is the northwest of Algeria located between latitudes (34°N, 37°N) and longitudes (2°W, 3°E). As explained above, the region *R* should be divided into several seismic zones. To do so, for each point *p* on the region, the punctual annual frequency of earthquakes is computed. For each point *p*, it is necessary to determine for every event *v* in the catalog if that event *v* could be perceived or not by human form point *p*. Thus the used formula is the one developed in **(McCue, 1980)** which provides an empirical relationship between earthquakes of various magnitudes and the radial distance over which the effects of that earthquake should be felt by people:

$$radius \simeq e^{\frac{M_L}{1.01} - 0.13} \tag{14}$$

For example, an earthquake of magnitude M_L = 3.3 could be felt by people in a radius of 23 km. The appli-

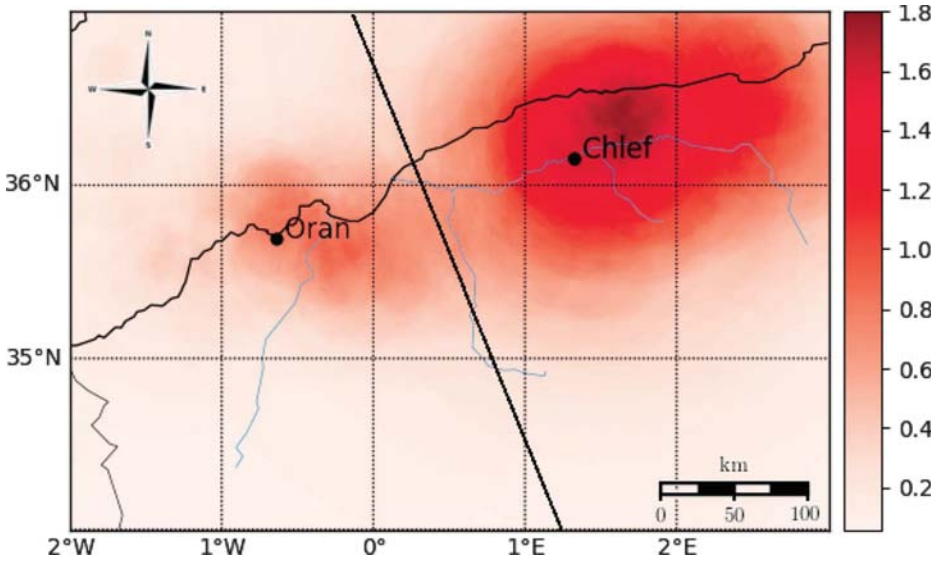

Figure 9: Distribution of the annual seismic frequency based on the McCue formula

cation of this method in the considered region allows us to distinguish mainly two active seismic zones (see **Figure 9**):

- z_1: the city of Oran (35° 41' 27''N, 0° 38' 30''W) and its surroundings, and
- z_2: the city of Chlef (36° 9 ' 54''N, 1° 20' 4''E) and its surroundings.

Based on this zoning, the Markov chain state space will be composed of four states described in **Table 3**.

Table 3: The different states of the Markov chain $E = \{e_\varphi, e_{Oran}, e_{Chle\ f}, e_{All}\}$

Global States	Zones States	Description
e_φ	$[z_1 = 0, z_2 = 0]$	The whole region is seismically quiet
eOran	$[z_1 = 1, z_2 = 0]$	The zone of Oran is active and that of Chlef is calm
eChle f	$[z_1 = 0, z_2 = 1]$	The zone of Oran is calm and that of Chlef is active
eAll	$[z_1 = 1, z_2 = 1]$	Both zones are seismically active

5. Temporal analysis

In general, e_φ which is the state defined by $e_\varphi = [z_1 = 0, z_2 = 0,..., z_n = 0]$ represents the state in which no zone in region R presents the occurrence of an earthquake. As well, e_{All} which is the state defined by $e_{All} = [z_1 = 1, z_2 = 1,..., z_n = 1]$ represents the state in which all zones of region R presents an occurrence of an earthquake. Time unit Δt was defined as the time interval used to sample the total period T. When Δt is too high, the probability of having earthquakes in all the zones z_i increases. When Δt is too small, the probability of having no earthquakes in

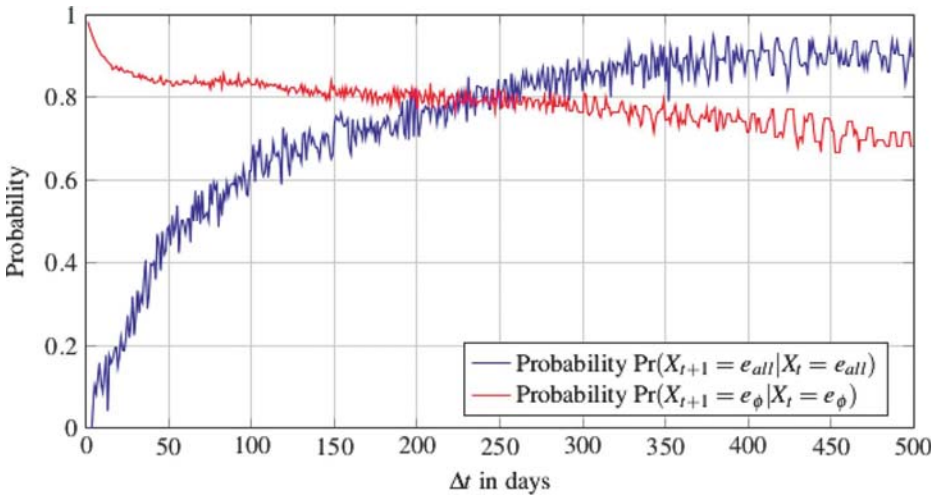

Figure 10: The relationship between Δt, Pr ($X_{t+1} = e_\varphi \mid X_t = e_\varphi$) and Pr ($X_{t+1} = e_{All} \mid X_t = e_{All}$).

any zones increases. Therefore, if Δt decreases Pr ($X_{t+1} = e_{\varphi} \mid X_t = e_{\varphi}$) increases, and if Δt increases Pr ($X_{t+1} = e_{All} \mid X_t = e_{All}$) increases. **Figure 10** shows the values of Pr ($X_{t+1} = e_{\varphi} \mid X_t = e_{\varphi}$) and Pr ($X_{t+1} = e_{All} \mid X_t = e_{All}$) for several values of Δt when building a Markov chain over the homogeneous catalogue for each value of Δt. According to a study conducted in **(Nava et al., 2005),** the most suitable value of Δt is the one that makes the two probabilities Pr ($X_{t+1} = e_{\varphi} \mid X_t = e_{\varphi}$) and Pr ($X_{t+1} = e_{All} \mid X_t = e_{All}$) as close as possible. This is represented by the point of intersection between the two curves in **Figure 10**. Thus, in conclusion Δt is chosen to be equal to **248 days**.

6. Application & Results

This section uses all the data and parameters defined in the previous sections to assess the probability of the occurrence of earthquakes in the future decades in each of the zones when using two models: the Poisson model and the Markov model.

6.1. Poisson model

The temporal occurrence of earthquakes is commonly described by a Poisson model, which is a simple model that assumes an independent event between the different earthquake occurrences. In this paper, the Poisson model is combined with the **(Gutenberg and Richter, 1956)** law to predict the probability of at least one exceedance of a particular earthquake of magnitude *m* in a period of t years by the expression:

$$\Pr(N \geq 1) = 1 - e^{-\lambda m \times t} \quad (15)$$

where N is the number of earthquakes of magnitude larger than m, and λ_m is estimated from the a-value and the b-value evaluated from using the empirical application of Gutenberg–Richter law on the homogeneous and completed catalogue:

$$\lambda_m = 10^{a-b\times m} \quad (16)$$

New empirical relationships (see **Figures 11** and **12**) among the zone of Oran and Chlef are formulated as:

$$\log(\lambda_m) = -1.106 \times m + 4.688 \quad R^2 = 0.992 \quad (17)$$

$$\log(\lambda_m) = -1.058 \times m + 4.811 \quad R^2 = 0.989 \quad (18)$$

Formula 15 was used to predict the probability of the occurrence of at least one earthquake of local magnitude greater than 5. The results are presented in **Figures 14** and **15**.

6.2. Markov model

Based on the methodology described in the previous sections a Markov chain is built according to the parameters showed in **Table 4**.

Indeed, **Figure 13** presents the transition graph of the obtained Markov chain. To understand the graph given in **Figure 13**, some explanations must be given:

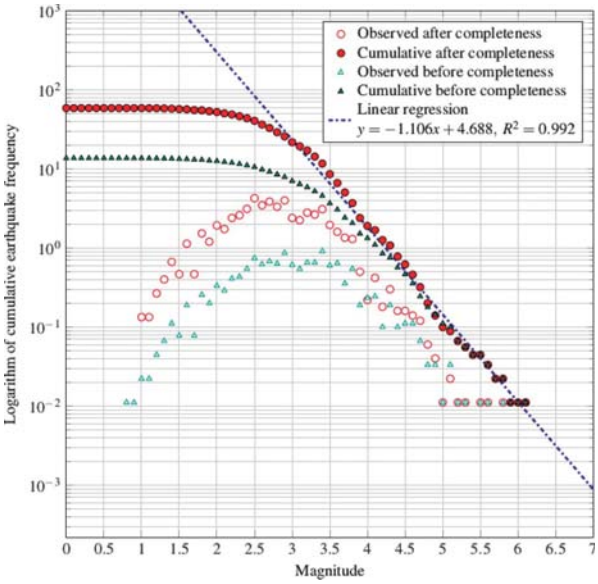

Figure 11: Gutenberg Richter law for the Oran zone z_o

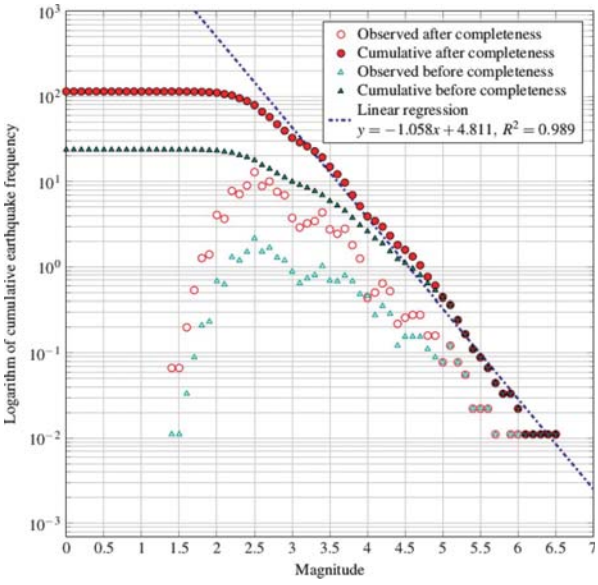

Figure 12: Gutenberg Richter law for the Chlef zone z_1

Table 4: Different parameters of the Markov chain

Parameter	Symbol	Value
Number of States	E	$\{e_{\varphi}, e_{Oran}, e_{Chle\ f}, e_{All}\}$
Magnitude threshold of completeness	M_c	2.5
Magnitude threshold	ε	3.5
Time unit	Δt	248 days
Period of time	T	1928 − 2018

- Each vertex of the graph represents a possible state of the system.
- The loop of the first vertex e_{All} labelled with the value 0.79 expresses the probability of the occur-

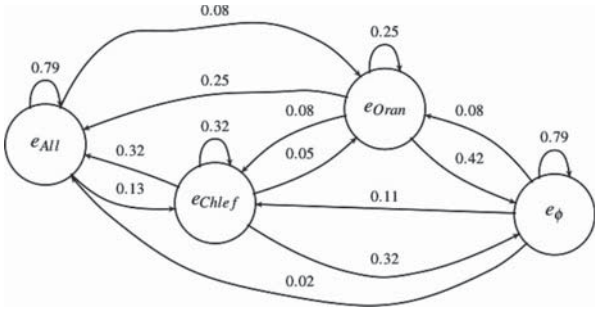

Figure 13: Obtained Markov chain

rence of earthquakes in both zones the next unit of time (Δt=*248* days) where some earthquakes were observed before in the unit of time, in both zones.

- The loop of the second vertex e_{Chlef} labelled with the value 0.32 expresses the probability of the occurrence of an earthquake in the zone of Chlef in the next unit of time where some earthquakes were observed before in the unit of time in the same zone.
- The loop of the third vertex e_{Oran} labelled with the value 0.25 expresses the probability of the occurrence of an earthquake in the zone of Oran in the next unit of time where some earthquakes were observed before in the unit of time in the same zone.
- The loop of the last vertex e_{φ} labelled with the value 0.79 expresses the probability of the absence of the occurrence of an earthquake in the next unit of time knowing that no earthquake was observed in the unit of time before.
- The transition labelled with the value 0.11 expresses the probability of the occurrence of an earthquake only in the zone of Oran during the next unit of time where no earthquake was observed in the unit of time before.
- The transition labelled with the value 0.32 expresses the probability of the absence of earthquakes in all the regions during the next unit of time where some earthquakes were observed in the unit of time before only in Oran.

The following matrix shows the transition matrix of the obtained Markov chain. It includes the various possible transition probabilities and it implies an equilibrium equation system that allows us to evaluate the stationary probabilities:

$$(\pi_{\varphi}, \pi_{Oran}, \pi_{Chlef}, \pi_{All}) \tag{19}$$

$$\begin{array}{c} \\ e_{\varphi} \\ e_{Oran} \\ e_{Chlef} \\ e_{All} \end{array} \begin{array}{c} \begin{array}{cccc} e_{\varphi} & e_{Oran} & e_{Chlef} & e_{All} \end{array} \\ \begin{pmatrix} 0.79 & 0.08 & 0.11 & 0.02 \\ 0.42 & 0.25 & 0.08 & 0.32 \\ 0.32 & 0.05 & 0.32 & 0.32 \\ 0.00 & 0.08 & 0.13 & 0.79 \end{pmatrix} \end{array} \Rightarrow$$

$$\Rightarrow \begin{cases} \pi_{\varphi} = 0.79\pi_{\varphi} + 0.42\pi_{Oran} + 0.32\pi_{Chlef} \\ \pi_{Oran} = 0.08\pi_{\varphi} + 0.25\pi_{Oran} + 0.05\pi_{Chlef} + 0.08\pi_{All} \\ \pi_{Chlef} = 0.11\pi_{\varphi} + 0.08\pi_{Oran} + 0.32\pi_{Chlef} + 0.13\pi_{All} \\ \pi_{All} = 0.02\pi_{\varphi} + 0.25\pi_{Oran} + 0.32\pi_{Chlef} + 0.79\pi_{All} \\ 1 = \pi_{\varphi} + \pi_{Oran} + \pi_{Chlef} + \pi_{All} \end{cases}$$

$$(\pi_{\varphi} \simeq 0.36,\ \pi_{Oran} \simeq 0.10,\ \pi_{Chlef} \simeq 0.14,\ \pi_{All} \simeq 0.40) \tag{20}$$

The transition matrix will be used to predict the probability of the occurrence of important earthquakes in each of the studied zones by simulating the Markov chain over 10^5 path.

For the zone of Oran (respectively Chlef) **Figure 14** (respectively **Figure 15**) shows the evolution of the probability of the occurrence of an earthquake of a local magnitude greater than 5 when assuming that no earthquakes (of magnitude greater than 5) were observed during the year of 2018 ($\Pr(e_{\varphi}) = 1$).

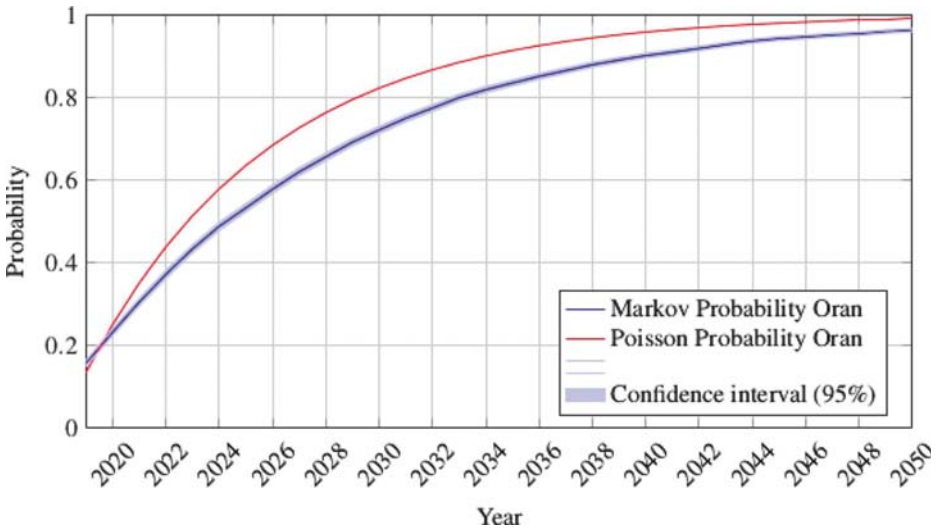

Figure 14: Poisson and Markov prediction in the region of Oran

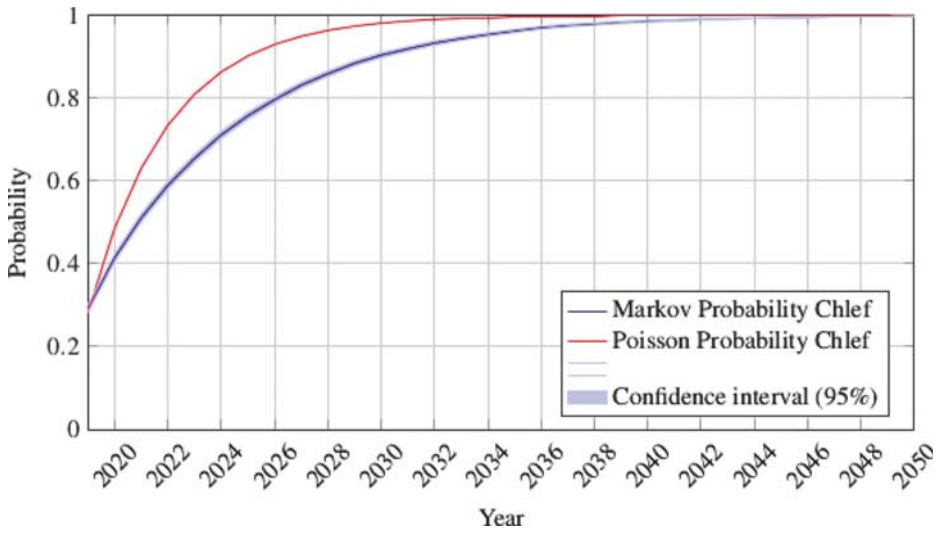

Figure 15: Poisson and Markov prediction in the region of Chlef

For both zones, the results show that both models (the Poisson model and the Markov model) predict a rapid growth of the probability of occurrences of earthquakes. It is noted that the Poisson model overestimates this probability compared to the Markov model. Through a period of prediction of one century, the average of this overestimation is about 3% for the zone of Oran and about 2% for the region of Chlef.

The results also show that the region of Chlef is more risky than the region of Oran. For both models, in the region of Oran the model described in this paper predicts a chance bigger than 80% to have an earthquake of a local magnitude greater than 5 after the year of 2033. This chance is more than 99% after the year of 2063. In the region of Chlef, after the year of 2026, an estimation to have an earthquake of a local magnitude greater than 5 is estimated to a likelihood bigger than 80%. This likelihood is more than 99% after the year of 2042.

7. Conclusion

Geological, and particularly, seismic hazards in Northwestern Algeria remain an area of research that needs to be studied by other approaches and methods in order to enrich the results. Indeed, in this paper, this work is based on the concept of the Markov chain to estimate seismic activity in the coming years by using the seismic history of the last century. An important part of the work was devoted to the homogenization and the completeness of the data.

The use of Markov chain allowed us to make probabilistic predictions of earthquakes for the next decade. The presence of two seismically active areas is noticed: one is located in Oran and another one in Chlef. It has also been noticed that the recent seismic activity is more concentrated in Chlef. Thus, this region has a high vulnerability compared to the rest of Northwest Algeria. Notice that the present results are consistent with the seismic hazard assessment of North Algeria reported in **(Aoudia et al., 2000), (Montilla et al., 2003), (Peláez et al., 2005), and (Mourabit et al., 2014)**.

The reported estimation of hazards shows that the region of Chlef presents a high to a very high hazard, however the region of Oran presents a moderate hazard.

More generally, the results show that the region of Northwestern Algeria is exposed to an important seismic risk in the coming few decades both in the region of Chlef and also the region of Oran.

8. References

Aki, K. (1984). Asperities, barriers, characteristic earthquakes and strong motion prediction. Journal of Geophysical Research: Solid Earth -89, B7, 5867-5872.

Anderson, D. L. and Whitcomb, J. H. (1973). The dilatancy-diffusion model of earthquake prediction. In Proceedings of the Conference on Tectonic Problems of the San Andreas Fault System, Stanford University Press Palo Alto, Calif. -13, 417-426.

Aoudia, A., Vaccari, F., Suhadolc, P., and Meghraoui, M. (2000). Seismogenic potential and earthquake hazard assessment in the tell atlas of algeria. Journal of Seismology - 4, 1, 79-98.

Bakun, W. H. and Lindh, A. G. (1985). The parkfield, california, earthquake prediction experiment. Science -229, 4714, 619-624.

Benouar, D. et al. (1994). Materials for the investigation of the seismicity of Algeria and adjacent regions during the twentieth century. Editrice Compositori, 416 p.

Beyreuther, M., Hammer, C., Wassermann, J., Ohrnberger, M., and Megies, T. (2012). Constructing a hidden markov model based earthquake detector: application to induced seismicity. Geophysical Journal International -189, 1, 602-610.

Beyreuther, M. and Wassermann, J. (2008). Continuous earthquake detection and classification using discrete hidden markov models. Geophysical Journal International, -175, 3, 1055-1066.

Bhargava, N., Katiyar, V., Sharma, M., and Pradhan, P. (2009). Earthquake prediction through animal behavior: A review. Indian J. Biomech -78, 159-165.

Bouhadad, Y. and Laouami, N. (2002). Earthquake hazard assessment in the oran region (northwest algeria). Natural Hazards – 26, 3, 227-243.

Brumbaugh, D. (1989). A comparison of duration magnitude to local magnitude for seismic events recorded in northern arizona. Journal of the Arizona-Nevada Academy of Science, 29-31.

Buforn, E., Coca, P., Udías, A., and Bezzeghoud, M. (2017). The Oran (Northwest Algeria) earthquake of 9 October 1790. In EGU General Assembly Conference Abstracts -19, 2005.

Caputo, M. (1974). Analysis of seismic risk. Nato Advanced Study Institutes Series, Appl Sci – 3, 55-86.

CGS (1995). The Benichougrane earthquake of August 18, 1994. Centre National de Recherche Appliquée en Génie Parasismique, Algérie, 40 p.

Chambers, D. W., Baglivo, J. A., Ebel, J. E., and Kafka, A. L. (2012). Earthquake forecasting using hidden markov models. Pure and applied geophysics -169, 4, 625-639.

Chen, Q. H. and Liu, Z. (2013). Earthquake magnitude prediction model based on the gep algorithm and markov chain.

In Applied Mechanics and Materials, Trans Tech Publ – 411, 2130-2133.

Chyi, L., Quick, T., Yang, T., and Chen, C. (2003). Soil gas radon spectra and earthquake prediction. In Proceedings of ICGG7, 31-32.

Cornell, C. A. (1968). Engineering seismic risk analysis. Bulletin of the Seismological Society of America, -58, 5, 1583-1606.

Cornell, C. A. and Vanmarcke, E. H. (1969). The major influences on seismic risk. In Proceedings of the Fourth World Conference on Earthquake Engineering -1, 69-83.

Der Kiureghian, A. and Ang, A. H. (1977). A fault-rupture model for seismic risk analysis. Bulletin of the Seismological Society of America – 67, 4, 1173-1194.

Déverchère, J., Yelles, K., Domzig, A., Mercier de Lépinay, B., Bouillin, J.-P., Gaullier, V., Bracène, R., Calais, E., Savoye, B., Kherroubi, A., et al. (2005). Active thrust faulting offshore boumerdes, algeria, and its relations to the 2003 mw 6.9 earthquake. Geophysical research letters -32, 4, 1-5.

Dewey, J. W. (1991). The 1954 and 1980 algerian earthquakes: Implications for the characteristic-displacement model of fault behavior. Bulletin of the Seismological Society of America -81, 2, 446-467.

Eftaxias, K., Kapiris, P., Polygiannakis, J., Bogris, N., Kopanas, J., Antonopoulos, G., Peratzakis, A., and Hadjicontis, V. (2001). Signature of pending earthquake from electromagnetic anomalies. Geophysical Research Letters, -28, 17, 3321-3324.

Gutenberg, B. and Richter, C. (1956). Magnitude and energy of earthquakes. Annals of Geophysics – 9, 1, 1-15.

Harbi, A., Peresan, A., and Panza, G. F. (2010). Seismicity of eastern algeria: a revised and extended earthquake catalogue. Natural hazards -54, 3, 725-747.

Heinicke, J., Koch, U., and Martinelli, G. (1995). Co2 and radon measurements in the vogtland area (germany)-a contribution to earthquake prediction research. Geophysical research letters -22, 7, 771-774.

Holliday, J. R., Nanjo, K. Z., Tiampo, K. F., Rundle, J. B., and Turcotte, D. L. (2005). Earthquake forecasting and its verification. Nonlinear Processes in Geophysics -12, 965-977.

Jackson, D. and Kagan, Y. (2006). The 2004 parkfield earthquake, the 1985 prediction, and characteristic earthquakes: Lessons for the future. Bulletin of the Seismological Society of America -96, 4B, S397-S409.

King, C.-Y. (1986). Gas geochemistry applied to earthquake prediction: An overview. Journal of Geophysical Research: Solid Earth – 91, B12, 12269-12281.

Knopoff, L. (1971). A stochastic model for the occurrence of main-sequence earthquakes. Reviews of Geophysics-9, 1, 175-188.

Kramer, S. L. (1996). Geotechnical Earthquake Engineering. Prentice-Hall, Upper Saddle River, New Jersey, 653 p.

Liu, S. and Fagel, L. (1972). Earthquake environment for physical design: A statistical analysis. Bell System Technical Journal -51, 9, 1957-1982.

Lomnitz-Adler, J. (1983). A statistical model of the earthquake process. Bulletin of the Seismological Society of America -73, 3, 853-862.

Lott, D. F., Hart, B. L., and Howell, M. W. (1981). Retrospective studies of unusual animal behavior as an earthquake predictor. Geophysical Research Letters – 8, 12, 1203-1206.

Markov, A. A. (1906). Rasprostranenie zakona bol'shih chisel na velichiny, zavisyaschie drug ot druga.

Izvestiya Fiziko-matematicheskogo obschestva pri Kazanskom universitete -15, 135-156.

Matthews, M. V., Ellsworth, W. L., and Reasenberg, P. A. (2002). A brownian model for recurrent earthquakes.

Bulletin of the Seismological Society of America – 92, 6, 2233-2250.

McCue, K. (1980). Magnitude of some early earthquakes in southeastern australia. Search -11, 3, 78-80.

McKenzie, D. (1972). Active tectonics of the mediterranean region. Geophysical Journal International -30,2, 109-185.

Meghraoui, M. (1988). Géologie des zones sismiques du Nord de l'Algérie: Paléosismologie, tectonique active et synthèse sismotectonique. PhD thesis, Paris 11, 355p.

Meghraoui, M., Morel, J.-L., Andrieux, J., and Dahmani, M. (1996). Tectonique plio-quaternaire de la chaine tello-rifaine et de la mer d'alboran; une zone complexe de convergence continent-continent. Bulletin de la Société géologique de France -167, 1, 141-157.

Merz, H. A. and Cornell, C. A. (1973). Seismic risk analysis based on a quadratic magnitude-frequency law. Bulletin of the Seismological Society of America – 63, 6, 1, 1999-2006.

Mogi, K. (1981). Seismicity in western japan and long-term earthquake forecasting. Earthquake prediction: An international review -4, 43-51.

Montilla, J. A. P., Hamdache, M., and Casado, C. L. (2003). Seismic hazard in northern algeria using spatially smoothed seismicity. results for peak ground acceleration. Tectonophysics -372, 1, 2, 105-119.

Mourabit, T., Elenean, K. A., Ayadi, A., Benouar, D., Suleman, A. B., Bezzeghoud, M., Cheddadi, A., Chourak, M., ElGabry, M., Harbi, A., et al. (2014). Neo-deterministic seismic hazard assessment in north africa. Journal of seismology -18, 2, 301-318.

Nava, F. A., Herrera, C., Frez, J., and Glowacka, E. (2005). Seismic hazard evaluation using markov chains: Application to the japan area. pure and applied geophysics -162, 6, 7, 1347-1366.

Nicholson, C. and Simpson, D. W. (1985). Changes in vp/vs with depth: Implications for appropriate velocity models, improved earthquake locations, and material properties of the upper crust. Bulletin of the Seismological Society of America -75, 4, 1105-1123.

Nur, A. (1974). Matsushiro, japan, earthquake swarm: Confirmation of the dilatancy-fluid diffusion model. Geology -2, 5, 217-221.

Peláez, J. A., Hamdache, M., and Casado, C. L. (2005). Updating the probabilistic seismic hazard values of northern algeria with the 21 may 2003 m 6.8 algiers earthquake included. pure and applied geophysics -162, 11, 2163-2177.

Peresan, A., Kossobokov, V., Romashkova, L., and Panza, G. (2005). Intermediate-term middle-range earthquake predictions in italy: a review. Earth-Science Reviews -69, 1, 2, 97-132.

Philip, H. (1987). Plio-quaternary evolution of the stress field in mediterranean zones of subduction and collision, Annals Of Geophysics, 301-320.

Philip, H. and Meghraoui, M. (1983). Structural analysis and interpretation of the surface deformations of the el asnam earthquake of october 10, 1980. Tectonics -2, 1, 17-49.

Philip, H. and Thomas, G. (1977). Détermination de la direction de raccourcissement de la phase de compression quaternaire en oranie (algérie). Rev. Geogr. Phys. Geol. Dynam -19, 315-324.

Quang, P. B., Gaillard, P., Cano, Y., and Ulzibat, M. (2015). Detection and classification of seismic events with progressive multi-channel correlation and hidden markov models. Computers & Geosciences -83, 110-119.

Rong, Y., Jackson, D. D., and Kagan, Y. Y. (2003). Seismic gaps and earthquakes. Journal of Geophysical Research: Solid Earth -108, B10, 1-14.

Schenková, Z. and Kárník, V. (1970). The probability of occurrence of largest earthquqkes in the european area – part ii. pure and applied geophysics -80, 1, 152-161.

Seeber, L. and Armbruster, J. G. (1981). Great detachment earthquakes along the himalayan arc and long-term forecasting. Earthquake prediction: an international review -4, 259-277.

Serpil, U. and CELEBIOGLU, S. (2011). Aa markov chain modelling of the earthquakes occuring in turkey. Gazi University Journal of Science -24, 2, 263-274.

Sonley, E. and Atkinson, G. M. (2005). Empirical relationship between moment magnitude and nuttli magnitude for small-magnitude earthquakes in southeastern canada. Seismological Research Letters -76, 6, 752-755.

Stepp, J. (1972). Analysis of completeness of the earthquake sample in the puget sound area and its effect on statistical estimates of earthquake hazard. In Proc. of the 1st Int. Conf. on Microzonazion, Seattle -2, 897-910.

Thomas, G. (1985). Géodynamique d'un bassin intramontagneux: Le Bassin du Bas-Chelif occidental (Algérie) durant le mio-plio-quaternaire. PhD thesis, Univ. Pau, 594 p.

Uyeda, S., Nagao, T., and Kamogawa, M. (2009). Short-term earthquake prediction: Current status of seismo-electromagnetics. Tectonophysics -470, 3, 4, 205-213.

Vagliente, V. N. (1973). Forecasting the risk inherent in earthquake resistant design. PhD thesis, Department of Civil Engineering, Stanford University, 244 p.

Veneziano, D. and Cornell, C. A. (1974). Earthquake models with spatial and temporal memory for engineering seismic risk analysis. MIT Department of Civil Engineering, 74–78.

Vere-Jones, D. (1966). A markov model for aftershock occurence. pure and applied geophysics – 64, 1, 31-42.

Votsi, I., Tsaklidis, G., Limnios, N., Papadimitriou, E., and Vallianatos, F. (2013). A markov model for seismic hazard analysis along the hellenic subduction zone (greece). Bulletin of the Geological Society of Greece – 47, 3, 1376-1385.

Walia, V., Virk, H. S., Yang, T. F., Mahajan, S., Walia, M., Bajwa, B. S., et al. (2005). Earthquake prediction studies using radon as a precursor in nw himalayas, india: a case study. Terrestrial Atmospheric and Oceanic Sciences -16, 4, 775-804.

Wang, C.-y., Goodman, R. E., and Sundaram, P. (1975). Variations of vp and vs in granite premonitory to shear rupture and stick-slip sliding: Application to earthquake prediction. Geophysical Research Letters – 2, 8, 309-311.

Wiemer, S. and Wyss, M. (2000). Minimum magnitude of completeness in earthquake catalogs: Examples from Alaska, the western united states, and japan. Bulletin of the Seismological Society of America – 90, 4, 859-869.

SAŽETAK

Procjena seizmičkoga rizika na sjeverozapadu Alžira temeljena na Markovljevu modelu

Glavni je cilj bio razviti Markovljev model kojim se procjenjuje seizmički rizik na sjeverozapadu Alžira. To je područje već klasificirano u zonu umjerene do jake seizmičke aktivnosti ($M_L \geq 2.5$). U radu su potresni događaji stohastički modelirani, uporabom diskretnoga, vremenskoga, Markovljeva lanca s modelom konačnoga stanja. Takav model primijenjen je na skupu podataka koji je obuhvatio sve potrese zabilježene na sjeverozapadu Alžira, na 34°N, 37°N sjeverne širine te dužinama 2°W zapadno do 3°E istočno. Podatci su prikupljeni za razdoblje 1928. – 2018. Model je izgrađen preko homogenoga kataloga, a izračunana matrica vjerojatnosti može se koristiti za predviđanje potresa u narednim desetljećima. Kao kontrolni model korišten je Poissonov.

Ključne riječi:
seizmički rizici, Markovljev lanac, Poissonov model, potres, sjeverni Alžir

Authors contribution

This paper is a part of PhD research of the author **Badreddine Dahmoune** who led the research, compiled the seismic catalogue, wrote all computer programs to analyse the data, to compute and to simulate the model. The supervisors of the PhD thesis, **Hamidi Mansour** (Full Professor) initialized the idea and participated in the analysis of the results.